Vibrational Revivals and the Control of Photochemical Reactions

S. Meyer and V. Engel*

Institut für Physikalische Chemie, Universität Würzburg, Am Hubland, 97074 Würzburg, Germany

Received: April 10, 1997; In Final Form: July 28, 1997[⊗]

The short-time vibrational wave packet motion in a molecule with several vibrational degrees of freedom shows oscillatory behavior with the characteristic vibrational periods. For long times revivals will occur, i.e., the wave packet restores its initial form. For small vibrational coupling the revival times in the single modes are approximately those of the uncoupled nuclear motion. The fact that the revivals with respect to the single degrees of freedom occur at different times can be used to control the branching ratio between reaction channels by short-pulse electronic excitation at different times. A model of the HOD molecule is used to demonstrate this general scenario.

I. Introduction

The control of chemical reactions by selective laser excitation has fascinated researchers working in theoretical and experimental chemistry and physics.[1−3] From the different control schemes developed over the years, let us mention three of basic importance. The first approach uses interferences (Brumer−Shapiro scheme):[4,5] if a final state is prepared via different indistinguishable pathways, interference occurs and the population of the final state can be influenced by adjusting a relative phase to achieve constructive or destructive interference. This is nothing more than the famous two-slit experiment, and several experiments on molecular systems that employ the Brumer−Shapiro scheme have been reported in the literature.[6−14]

Another approach uses time-delayed ultrashort laserpulses (Tannor−Kosloff−Rice scheme):[15,16] a first pulse prepares a coherent superposition of molecular eigenstates, i.e., a wave packet which moves in time until, being localized in certain regions of space, the interaction with another short pulse yields selective reaction products. The principle of this scheme is also an interference phenomenon: a single fragment state can be accessed via a superposition of intermediate states which evolve in time, i.e., a wave packet. A first experiment which used time-delayed pulses to control the outcome of a laser excitation process was performed by Potter et al.[17] An experimental proof that the branching ratio beween different reaction channels can indeed be influenced using the above control-scheme was given by Baumert et al. who were able to control the Na_2^+ versus the $Na + Na^+$ signal in multiphoton ionization experiments on the sodium dimer.[18]

Revival phenomena have been studied, for example, in the context of the interaction of atoms with a quantized field,[19−21] the motion of atomic Rydberg wave packets,[22−25] and in rotational coherent spectroscopy.[26] This effect occurs in the time-evolution of a coherent superposition of quantum states which is prepared in a system at time $t = 0$. The time-dependent phase factors which determine the temporal change of the single states will dephase until at a time τ all factors have (approximately) the same phase relationship as at $t = 0$ and the resulting wave packet resembles the one prepared initially. Revivals of vibrational wave packets have been first observed for the Na_2 molecule.[27] Very detailed experiments on revivals and fractional revivals in vibrational dynamics of diatomic molecules have been presented lately by Stolow and co-workers.[28−30] For theoretical treatments see refs 31−34. In this paper we will show how vibrational revivals in a system with more than one degree of freedom can, in principle, be used to direct a dissociation process into a specific reaction channel. In this context it is irrelevant how the vibrational wave packet is prepared. The idea is similar to a recently presented isotope separation scheme.[35]

We use the $\tilde{A}^1B_1 \leftarrow \tilde{X}^1A_1$ electronical transition of HOD[36,37] to illustrate the effect described above. This is done within a model which has been used before to investigate the control of the H + OD/D + OH branching ratio.[38,39] The water molecule and its isotopes was also used to demonstrate another control scheme: beautiful experiments have been performed by Crim and co-workers[40−43] and others[44,45] who examined the photodissociation of water starting from different initial rotational−vibrational states. The variation of the laser wavelength and the initial bound-state results in a very large variation of the branching ratio and the fragment distributions. For related theoretical work on the dissociation of water see refs 46−50. The present work is related to the above-mentioned studies but here we are not interested in the optimization of particular reaction yields, rather it will be shown that, quite generally, the long-time dynamics of more-dimensional vibrational wave packets automatically will result in specific branching ratios of fragments if an electronic transition to an antibonding state is induced by time-delayed short-pulse excitation.

Section 2 discusses the vibrational wave packet dynamics and more-dimensional revivals within a simplified model. In section 3 UV excitation using a wave packet of HOD in its electronic ground state as initial state is discussed and the branching ratio between fragments in the reaction channels H + OD and D + OH is calculated. A summary and conclusion is given in section 4.

II. Two-Dimensional Revivals

In this section we discuss the dynamics of a general vibrational wave packet for the specific case of the two-dimensional motion within the electronic ground state $|g\rangle$ of the HOD molecule (the $\tilde{X}^1A_1$ state). In our restricted model, the bond angle is fixed to its value at equilibrium $\gamma = 104°$ and the Hamiltonian for the vibrational motion in the OH coordinate r_H and the OD coordinate r_D is parametrized in the form (atomic units are used)

[⊗] Abstract published in *Advance ACS Abstracts,* September 15, 1997.

S1089-5639(97)01247-4 CCC: $14.00

$$H_g(r_H, r_D) = -\frac{1}{2\mu_H}\frac{\partial^2}{\partial r_H^2} - \frac{1}{2\mu_D}\frac{\partial^2}{\partial r_D^2} - \frac{\cos\gamma}{m_O}\frac{\partial^2}{\partial r_H \partial r_D} + V_g(r_H, r_D) \quad (1)$$

were μ_H and μ_D denote the reduced masses of OH and OD and m_O is the oxygen mass. The potential is given by

$$V_g(r_H, r_D) = D(1 - e^{-\beta(r_H - r_0)})^2 + D(1 - e^{-\beta(r_D - r_0)})^2 - \frac{A(r_H - r_0)(r_D - r_0)}{1 + e^{((r_H - r_0) + (r_D - r_0))}} \quad (2)$$

with the parameters $D = 0.2092$, $\beta = 1.1327$, $r_0 = 1.81$, and $A = 0.006\,76$, everything given in atomic units. This model potential was taken from ref 51, and it was employed in other model studies of the $\tilde{A} \leftarrow \tilde{X}$ transition of the water molecule.[38,39,52,53] The freezing of the bond angle to its value at equilibrium is indeed a very good approximation for the electronical excitation which is regarded here.[54,55] Note, however, that the anisotropy of the electronic $\tilde{B}^1A_1$ state of water is very large around the angle $\gamma = 104°$ so that for the $\tilde{B} \leftarrow \tilde{X}$ transition the rotational degree of freedom cannot be neglected.[56,57]

Let us assume that a wave packet in the state $|g\rangle$ is prepared. This can be achieved, for example, by strong-pulse infrared excitation or multiphoton transitions via excited electronic states, see section 3. The wave packet is a coherent superposition of stationary eigenstates φ_n with eigenenergies E_n:

$$\psi(r_H, r_D, t) = \sum_n a_n \varphi_n(r_H, r_D) e^{-iE_n t} \quad (3)$$

where n collects all vibrational quantum numbers. For the moment we will disregard the coupling between the vibrational modes and concentrate on the one-dimensional wave packet motion in the respective bond coordinates. These motions are described by the functions:

$$\psi_\alpha(r_\alpha, t) = \sum_{n_\alpha} a_{n_\alpha} e^{-iE_{n_\alpha} t} \varphi_{n_\alpha}(r_\alpha) \quad (4)$$

with $\alpha = H$ or D. The energies and functions which appear in this equation correspond to the OH ($\alpha = H$) and OD ($\alpha = D$) vibrational motion, respectively. Regarding a single vibrational degree of freedom separately we will find the characteristics of a one-dimensional bound-state motion. For nonharmonic potentials the initially localized wave packet will disperse and show vibrational revivals after a revival time τ_α. This time can be calculated analytically if the single-mode Hamiltonians contain Morse potentials so that the vibrational eigenenergies can be expressed as a polynomial of degree two in the quantum numbers n_α:

$$E_\alpha = a_\alpha(n_\alpha + {}^1/_2) - b_\alpha(n_\alpha + {}^1/_2)^2 \quad (5)$$

with $a_\alpha = \beta\sqrt{2D/\mu_\alpha}$, $b_\alpha = \beta^2/(2\,\mu_\alpha)$, and β and D are the Morse parameters. If the wave packet is a superposition of states with energies around an average energy E_m, the revival time τ can be calculated as

$$\tau = \frac{T(m+1,m)T(m,m-1)}{T(m+1,m) - T(m,m-1)} \quad (6)$$

where $T(m,m') = 2\pi/(E_m - E_{m'})$ is the classical period corresponding to the energy difference between two levels. In the case of the Morse oscillator one finds $\tau = \pi/b_\alpha$. If higher order terms are included in the expansion (eq 5) it is still possible to find analytical expressions for revival times.[32−34] For the two approximately uncoupled vibrations in our model system there will be two revival times τ_H and τ_D corresponding to the OH and OD vibrational motion, respectively. With the parametrization of eq 2 we find $\tau_H \sim 201$ fs and $\tau_D \sim 380$ fs. At times around τ_H the wave packet $\psi(r_H, r_D, t)$ will, if the vibrational coupling is not too strong, be localized in the r_H coordinate and not necessarily be localized in the r_D coordinate. The opposite holds for the wave packet at times which are close to τ_D. However, in the present case, the second revival of the OH motion occurs around the first OD revival since (for the Morse oscillator) the revival time scales directly with the molecular mass. To get an estimate of the relevant time scales of our problem, we calculated the time evolution of one-dimensional wave packets for the OH and OD motion using the Morse potential given in eq 2. The time propagation was performed within the split-operator method.[58,59] Figure 1 shows the modulus of the autocorrelation functions

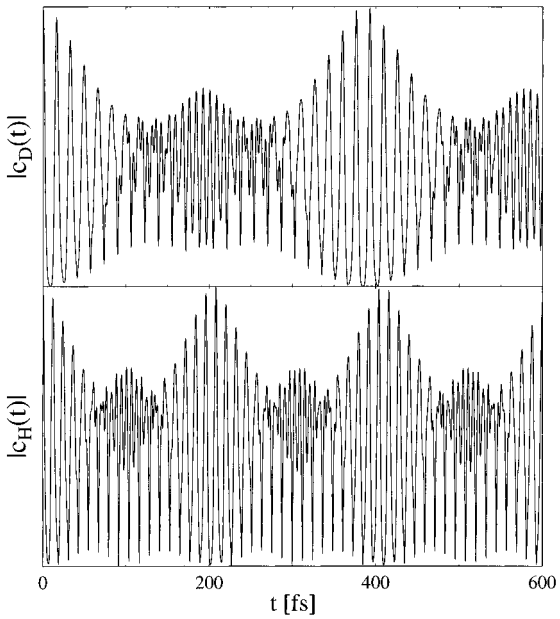

Figure 1. The autocorrelation function (eq 7) for the OD and OH one-dimensional vibrational motion.

$$c_\alpha(t) = \int dr_\alpha \psi_\alpha(0)\psi_\alpha(t) \quad (7)$$

Here the initial state $\psi_\alpha(0)$ was the respective vibrational ground-state shifted by $\Delta r_\alpha = 1.8$ au to larger distances. The fast oscillations of the functions correspond to the periods of the OH (∼17 fs) and OD (∼12 fs) molecule. As estimated above revivals occur around 200 fs (OH) and 400 fs (OD). Also, the fractional revivals (around $\tau_\alpha/2$) with the double vibrational periods can be seen in the figure whereas higher order fractional revivals are not seen.

III. UV Excitation

We now regard bound-free transitions $|e\rangle \leftarrow |g\rangle$ between the electronical ground state $|g\rangle(\tilde{X})$ and first excited state $|e\rangle(\tilde{A})$ of the HOD molecule. The $\tilde{A}$ state is purely antibonding and results in fragments $H(^2S) + OD(X,^2\pi)$ or $D(^2S) + OH(X,^2\pi)$. The potential energy surface was calculated by Palma and Staemmler[60] and was used in the first complete ab initio study of the photodissociation of a triatomic molecule.[36,54]

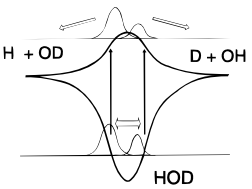

Figure 2. Sketch of the excitation scheme for the photodissociation of HOD, where the initial state is a vibrational wave packet in the electronic ground state. Cuts along the reaction coordinate defined by the minimum energy path of the antibonding excited-state potential are shown.

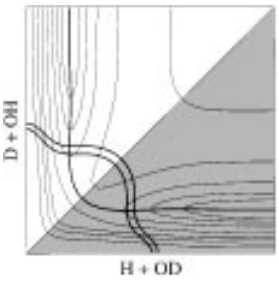

Figure 3. Potential energy surface for the $\tilde{A}$ state of water. Assigning the value zero to the lowest energy contour, contours with the values 0.0, 0.01, 0.03, 0.07, 0.13, 0.18, and 0.28 au are shown. The bond lengths range from 1 to 5.725 au. The thick lines indicate the minimum energy path and the Franck−Condon window for an excitation frequency of 0.12 au. The two lines which mark the Franck−Condon window correspond to 0.11 and 0.13 au, respectively.

Assuming that a vibrational wave packet in the electronic ground state is prepared, what will happen if an UV-excitation to the electronic $|e\rangle$ state induced by a femtosecond pulse occurs at different times? Figure 2 contains a sketch of such an excitation scheme. Cuts along the reaction coordinate defined by the minimum energy path on the excited potential (see also Figure 3) are drawn for the excited and ground state. The vertical arrows symbolize the central frequency of the UV excitation laser. If a compact vibrational wave packet in the ground state is located left from the symmetry line, the D + OH channel will be populated preferentially; a location right from the symmetry line will result in a strong H + OD production. Let us be more specific and determine the spatial region where, for a given laser frequency ω, the excitation $|e\rangle \leftarrow |g\rangle$ will be most effective (the Franck−Condon window). This can be done within first-order perturbation theory which determines the nuclear wave function in the $|e\rangle$ state as

$$\psi_e(r_H,r_D,t) \sim \int_T^t dt'\, e^{-iH_e(t-t')}\mu_{eg}f(t')e^{-i\omega t'}\, e^{-iH_g(t'-T)}\psi_g(r_H,r_D,T) \quad (8)$$

where μ_{eg} is the projection of the transition dipole moment on the polarization vector of the laser and $f(t)$ is the envelope function of the laser pulse with frequency ω. H_e, H_g are the nuclear Hamiltonians for the excited and ground electronic states and $\psi_g(r_H,r_D,T)$ is the ground-state vibrational wave packet at the time T, when the laser pulse starts interacting with the molecule. Note that the wave function eq 8 depends on the delay time T. In eq 8 we have neglected unimportant factors and regard the $|e\rangle \rightarrow |g\rangle$ absorption process only. For short pulses we can neglect the kinetic energy operators under the integral[61−63] to obtain

$$\psi_e(r_H,r_D,t) = e^{-iH_e t}\mu_{eg}\psi_g(r_H,r_D,T)I(r_H,r_D,\omega) \quad (9)$$

with the Fourier integral

$$I(R_H,R_D,\omega) = \int_{-\infty}^{\infty} dt'\, e^{-i(V_e(r_H,r_D)-V_g(r_H,r_D)-\omega)t'}f(t') \quad (10)$$

Here we assumed that at time t the pulse envelope $f(t)$ has decreased to zero so that the integration range in eq 10 can be extended. The weighting function $I(r_H,r_D,\omega)$ defines the Franck−Condon window for resonant excitation. In particular it has its maximum modulus at points where

$$D(r_H,r_D) = V_e(r_H,r_D) - V_g(r_H,r_D) = \omega \quad (11)$$

The difference potential $D(R_H,R_D)$ is crucial for the intensity of spectroscopic transitions.[64] Figure 3 shows contours of the excited-state potential. The minimum energy path which connects the fragment channels via the reaction barrier is shown as well as the Franck−Condon window for a frequency of $\omega = 0.12$ au. The latter is symmetric and reaches into the fragmentation channels. A laser pulse with frequency ω is able to induce transitions to the excited state if parts of the initial state ψ_g are localized in the marked region. Since the initial state is nonstationary, the excitation efficiency depends on the time when the pulse starts interacting with the molecule.

Let us now look at the time-evolution of ψ_g around 200 fs, i.e., the revival time τ_H of the OH motion. The vibrational wave packet was prepared by simultaneous interaction of the molecule with two pulses of frequencies $\omega_1 = 0.28$ au and $\omega_2 = 0.12$ au and we assume them to be phase locked with zero relative phase. The calculation was done nonperturbatively so that the two electronic states are coupled by two laser fields.[65] The vibrational ground state was used as initial state and the transition-dipole moment was set to a constant. The latter (Condon) approximation is a good one if not very high vibrational initial states participate.[54] We took a $sin^2(t)$ with 12 fs fwhm for the pulse envelope function $f(t)$. The coupling strength μ_{eg} was set to 0.02 au. Since the transition dipole moment in the Franck−Condon region for the $|e\rangle \leftarrow |g\rangle$ transition is in the order of 1 D[54] this corresponds to a field intensity of around 10^{14} W/cm^2 which can be achieved with modern laser sources. The choice of the frequencies ω_1 and ω_2 is motivated as follows: first, we want an efficient population transfer induced by the pulse with ω_1 (corresponding to ∼165 nm) thus this frequency is chosen to be in the absorption maximum for the electronic transition. Second, to exceed higher vibrational states by the dump process, the second frequency has to be much smaller than the first one. If, on the other hand, it is chosen too small the Franck−Condon region for the stimulated emission process is located out in the reaction channels in a region which is passed very rapidly by the outgoing packets. This decreases the efficiency of the transition.

Figure 4 displays contours of the wave packet at different times. The shown time interval corresponds to one vibrational period of the OH uncoupled motion; note, however, that the calculation includes the coupling term between r_H and r_D. The figure shows that around τ_H the two-dimensional wave packet is localized in the r_H coordinate but not in the r_D coordinate. This is clearly seen at the times $t = 0$ fs and $t = 14$ fs. It is quite reasonable to expect that if a compact wave packet is located in the Franck−Condon window for the $|e\rangle \leftarrow |g\rangle$ transition at the time a pulse interacts with the molecule, the population transfer is more effective than if a smaller part of a delocalized packet serves as initial state for excitation (see eq 8). This should still be true for the finite width of the pulse which averages the motion of the initial state over a given time. Thus if the second pulse is fired at a delay-time, which is in the order of τ_H, we would expect that more OD fragments than OH fragments are built. This expectation is confirmed by a

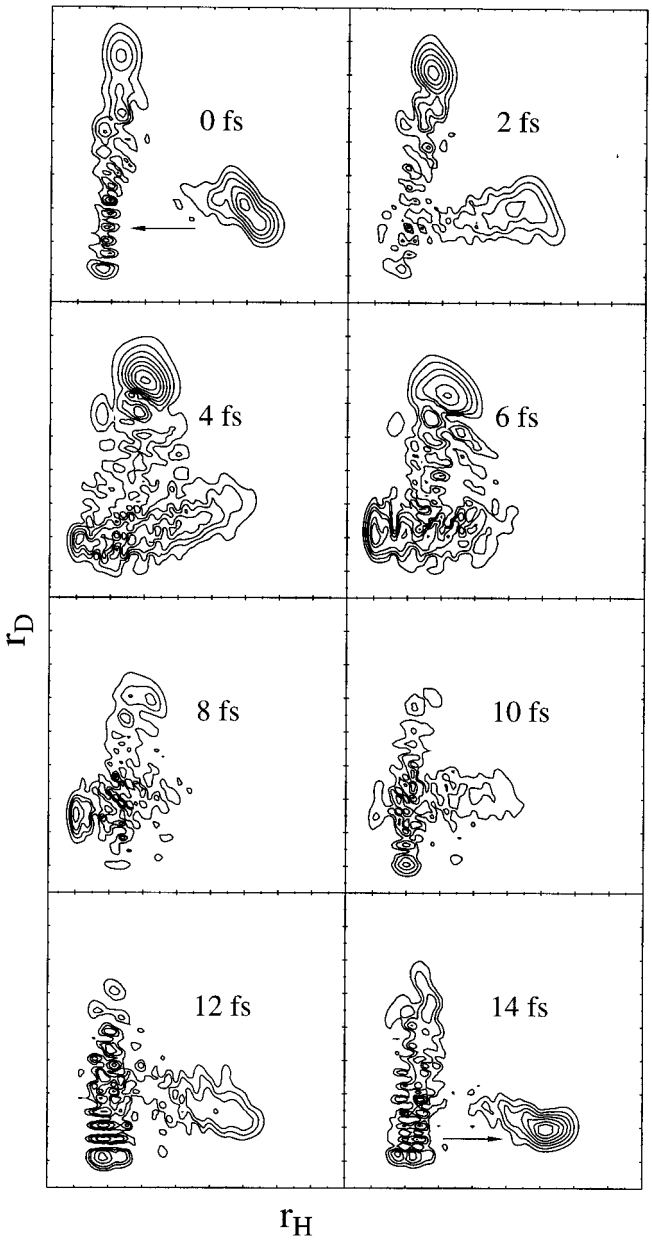

Figure 4. Vibrational wave packet dynamics in the ground electronic state of HOD. Shown are contours of the modulus squared of the packet at times around the revival time of the OH motion.

numerical calculation of the branching ratio as a function of the delay time T defined as

$$R_{H/D}(T) = \frac{|\psi_e(r_H \rightarrow \infty, r_D, t_{end})|^2}{|\psi_e(r_H, r_D \rightarrow \infty, t_{end})|^2} \qquad (12)$$

In practice, the final time t_{end} is chosen long enough so that the excitation process is finished and the two packets are located far out in the asymptotic reaction channels. Figure 5 contains the branching ratio which was calculated for delay times up to 550 fs. The curve shows oscillations around an average value of $R_{H/D} = 1.5$. If we choose a larger frequency ω_2, this average branching ratio stays the same, but because the ground state wave packet then consists mainly of the ground vibrational state, the deviation from this value is much smaller. Around the revival time of the OH motion (200 fs) we find a variation of the branching ratio between the values 1 and 5. The oscillations correspond to the vibrational period of OH which confirms what we reasoned above, namely, a localized wave packet in the OH

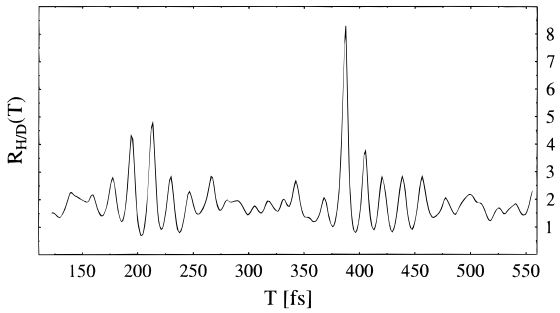

Figure 5. Branching ration $R_{H/D}(T)$ for the production of H and D atoms (eq 12) as a function of the time delay between two ultrashort laser pulses.

bond results in an increased yield of OD molecules upon laser excitation at selected times. Around 400 fs the wave packets in the OH and the OD coordinate are both localized since here OH has its second revival and OD its first one. This results in an even higher population of the H + OD channel. That this fragment channel is preferentially populated almost at all times can be understood within a classical picture. If we start classical trajectories with zero initial momenta in the Franck−Condon window on the upper surface,[37] the accelerations $(\partial V_e/\partial r_\alpha)/m_\alpha$ along the r_H and r_D directions will determine the exit channel, i.e., if the acceleration along r_H direction is larger than along r_D the H + OD channel will be preferentially populated. Since the gradients along the two bond distances are equal, we obtain the ratio

$$\frac{m_D(\partial Ve/\partial r_H)}{m_H(\partial V_e/\partial r_D)} = \frac{m_D}{m_H} \sim 2 \qquad (13)$$

Thus the branching ration within this limit shoud be in the order of two which indeed is found for long pulse-photodissociation, for a more detailed discussion see ref 66. Of course this consideration neglects the details of the quantum mechanical laser excitation process.

Here we note that at very short delay times (several vibrational periods) the branching ratio also varies strongly with time which is reasonable since the preparation process creates a wave packet which is localized for a short time after the molecule−field interaction stopped.

The present calculation uses a single initial vibrational state of the HOD molecule. If an experiment is performed on hot samples we would have to Boltzmann average our results over all populated initial states. We expect that overall rotation of the molecule will not influence the effect we have described above. The transitions starting from excited vibrational states, which are populated less than the ground state, should show the same behavior as the transition starting from the ground state since the only situation which is needed for the revivals to occur is the production of a localized wave packet within the ground-state vibrational manifold.

Another comment is in order here. We regarded the preparation of a ground-state wave packet via a dissociative intermediate state. Since the fragmentation presents a loss mechanism, it is much more efficient to use a bound intermediate state for the preparation process. This however needs photons with much higher frequency.

IV. Summary

In this paper we have shown that the revival behavior of more-dimensional vibrational wave packets can, in principle, be used to control the branching ration between different reaction channels by the use of time-delayed short-pulse excitation. Since

at the revival time in a single vibrational mode the wave packet is localized in the respective coordinate, excitation to electronically excited states is more effective. This is a quite general effect which however is not likely to be observed for large vibrational coupling. We used the HOD molecule as a numerical example but did not attempt to optimize the outcome of the photodissociation process. Nevertheless, a large variation of the population in the reaction channels could be obtained. The idea presented here is related to the work of Averbukh et al. who demonstrated that the branching ratio of different isotopes obtained by laser excitation depends on the revival behavior of the single isotopes. In our case we regard vibrational motion within an ensemble of molecules of the same species. Thus we are dealing with the coherent superposition of vibrational motion within different degrees of freedom and not with a statistical mixture. Here of course the strength of the vibrational coupling is crucial. For the future it will be worthwile to perform more elaborate studies on systems with more vibrational degrees of freedom and to investigate in detail the rôle of the mode coupling.

Financial support by the DFG within the Schwerpunktsprogramm, *Femtosecond excitation of atoms, molecules and clusters*, and by the Fonds der Chemischen Industrie is gratefully acknowledged. We thank Ch. Hotz and C. Meier for helpful discussions.

References and Notes

(1) Warren, W. S.; Rabitz, H.; Dahleh, M. *Science* **1993**, *259*, 1581.
(2) Manz, J.; Wöste, L., Eds. *Femtosecond Chemistry*; VCH: Weinheim, 1995.
(3) XXth Solvay Congress on Chemistry, Brussels, November 28 − December 2, 1995.
(4) Brumer, P.; Shapiro, M. *Chem. Phys. Lett.* **1986**, *126*, 541.
(5) Brumer, P.; Shapiro, M. *Annu. Rev. Phys. Chem.* **1992**, *43*, 257.
(6) Chen, C.; Yin, Y. Y.; Elliot, D. S. *Phys. Rev. Lett.* **1990**, *64*, 507.
(7) Chen, C.; Elliot, D. S. *Phys. Rev. Lett.* **1990**, *65*, 1737.
(8) Park, S. M.; Lu, S.-P.; Gordon, R. J. *J. Chem. Phys.* **1991**, *94*, 8622.
(9) Lu, S.-P.; Park, S. M.; Xie, Y.; Gordon, R. J. *J. Chem. Phys.* **1992**, *96*, 6613.
(10) Sheehy, B.; Walker, B.; DiMauro, L. F. *Phys. Rev. Lett.* **1995**, *74*, 4799.
(11) Kleiman, V. D.; Zhu, L.; Lie, X.; Gordon, R. J. *J. Chem. Phys.* **1995**, *102*, 5863.
(12) Kleiman, V. D.; Zhu, L.; Allen, J.; Gordon, R. J. *J. Chem. Phys.* **1995**, *103*, 10800.
(13) Zhu, L.; Kleiman, V. D.; Lie, X.; Lu, S.-P.; Trentelman, K.; Gordon, R. J. *Science* **1995**, *270*, 77.
(14) Garrett, W. R.; Zhu, Y. *J. Chem. Phys.* **1997**, *106*, 2045.
(15) Tannor, D. J.; Kosloff, R.; Rice, S. A. *J. Chem. Phys.* **1986**, *85*, 5805.
(16) Tannor, D. J.; Rice, S. A. *J. Chem. Phys.* **1985**, *83*, 501.
(17) Potter, E. D.; Herek, J. L.; Pedersen, S.; Liu, Q.; Zewail, A. H. *Nature* **1992**, *355*, 66.
(18) Baumert, T.; Gerber, G. *Adv. Mol. Opt. Phys.* **1995**, *35*, 163.
(19) Eberly, J. H.; Narozhny, N. B.; Sanchez-Mondragon, J. J. *Phys. Rev. Lett.* **1980**, *44*, 1323.
(20) Narozhny, N. B.; Sanchez-Mondragon, J. J.; Eberly, J. H. *Phys. Rev. A* **1981**, *23*, 236.
(21) Yoo, H. I.; Eberly, J. H. *Phys. Rep.* **1985**, *118*, 239.
(22) 10Wolde, A.; Noordam, L. D.; Lagendijk, A.; van Linden van den Heuvell, H. B. *Phys. Rev. A* **1989**, *40*, 485.
(23) Yeazell, J. A.; Mallalieu, M.; Stroud, C. R. *Phys. Rev. Lett.* **1990**, *64*, 2007.
(24) Meacher, D. R.; Meyler, P. E.; Hughes, I. G.; Ewart, P. *J. Phys. B: At., Mol. Phys.* **1991**, *24*, L63.
(25) Alber, G.; Zoller, P. *Phys. Rep.* **1991**, *199*, 231.
(26) Felker, P. M.; Zewail, A. H. In ref 2, Chapter 5.
(27) Baumert, T.; Engel, V.; Röttgermann, C.; Strunz, W. T.; Gerber, G. *Chem. Phys. Lett.* **1992**, *191*, 639.
(28) Fischer, I.; Villeneuve, D. M.; Vrakking, M. J. J.; Stolow, A. *J. Chem. Phys.* **1995**, *102*, 5566.
(29) Vrakking, M. J. J.; Villeneuve, D. M.; Stolow, A. *Phys. Rev. A* **1996**, *54*, R37.
(30) Fischer, I.; Vrakking, M. J. J.; Villeneuve, D. M.; Stolow, A. *Chem. Phys.* **1996**, *207*, 331.
(31) Averbukh, I. Sh.; Perel'man, N. F. *Phys. Lett. A* **1989**, *139*, 449.
(32) Knospe, O.; Schmidt, R. *Phys. Rev. A* **1996**, *54*, 1154.
(33) Leichtle, C.; Averbukh, I. Sh.; Schleich, W. P. *Phys. Rev. Lett.* **1996**, *77*, 3999.
(34) Leichtle, C.; Averbukh, I. Sh.; Schleich, W. P. *Phys. Rev. A* **1996**, *54*, 5299.
(35) Averbukh, I. Sh.; Vrakking, M. J. J.; Villeneuve, D. M.; Stolow, A. *Phys. Rev. Lett.* **1996**, *77*, 3518.
(36) Engel, V.; Staemmler, V.; Vander Wal, R. L.; Crim, F. F.; Sension, R. J.; Hudson, B.; Andresen, P.; Hennig, S.; Weide, K.; Schinke, R. *J. Phys. Chem.* **1992**, *96*, 3201.
(37) Schinke, R. *Photodissociation Dynamics*; Cambridge University Press: Cambridge, 1993.
(38) Amstrup, B.; Henriksen, N. E. *J. Chem. Phys.* **1992**, *97*, 8285.
(39) Henriksen, N. E.; Amstrup, B. *Chem. Phys. Lett.* **1993**, *213*, 65.
(40) Vander Wal, R. L.; Crim, F. F. *J. Phys. Chem.* **1989**, *93*, 5331.
(41) Vander Wal, R. L.; Scott, J. L.; Crim, F. F. *J. Chem. Phys.* **1990**, *92*, 803.
(42) Vander Wal, R. L.; Scott, J. L.; Crim, F. F. *J. Chem. Phys.* **1990**, *94*, 1859.
(43) Vander Wal, R. L.; Scott, J. L.; Crim, F. F.; Weide, K.; Schinke, R. *J. Chem. Phys.* **1991**, *94*, 3548.
(44) Cohen, Y.; Bar, I.; Rosenwaks, S. *Chem. Phys. Lett.* **1994**, *228*, 426.
(45) Cohen, Y.; Bar, I.; Rosenwaks, S. *J. Chem. Phys.* **1995**, *102*, 3612.
(46) Segev, E.; Shapiro, M. *J. Chem. Phys.* **1982**, *77*, 5604.
(47) Hartke, B.; Manz, J.; Mathis, J. *J. Chem. Phys.* **1989**, *139*, 123.
(48) Hartke, B.; Manz, J. *J. Chem. Phys.* **1990**, *92*, 220.
(49) Hartke, B.; Janza, A. E.; Karrlein, W.; Manz, J.; Mohan, V.; Schreier, H.-J. *J. Chem. Phys.* **1992**, *96*, 3569.
(50) Manz, J.; Paramonov, G. K. *J. Phys. Chem.* **1993**, *97*, 12625.
(51) Reimers, J. R.; Watts, R. O. *Mol. Phys.* **1984**, *52*, 357.
(52) Zhang, J.; Imre, D. G. *J. Chem. Phys.* **1989**, *90*, 1666.
(53) Zhang, J.; Imre, D. G.; Frederick, J. H. *J. Phys. Chem.* **1989**, *93*, 1840.
(54) Engel, V.; Schinke, R.; Staemmler, V. *J. Chem. Phys.* **1988**, *88*, 129.
(55) von Dirke, M.; Schinke, R. *Chem. Phys. Lett.* **1992**, *196*, 51.
(56) Weide, K.; Schinke, R. *J. Chem. Phys.* **1987**, *87*, 4627.
(57) Weide, K.; Schinke, R. *J. Chem. Phys.* **1989**, *90*, 7150.
(58) Fleck, J. A.; Morris, J. R.; Feit, M. D. *Appl. Phys.* **1976**, *10*, 129.
(59) Feit, M. D.; Fleck, J. A.; Steiger, A. *J. Comput. Phys.* **1982**, *47*, 412.
(60) Staemmler, V.; Palma, A. *Chem. Phys.* **1985**, *93*, 63.
(61) Braun, M.; Meier, C.; Engel, V. *J. Chem. Phys.* **1995**, *103*, 7907.
(62) Lee, S.-Y. *J. Chem. Phys.* **1982**, 76, 3064 ; Lee, S.-Y. In ref 2, Chapter 7.
(63) Smith, T. J.; Ungar, L. W.; Cina, J. A. *J. of Lumin.* **1994**, *58*, 66.
(64) Mulliken, R. S. *J. Chem. Phys.* **1971**, *55*, 309.
(65) Heather, R. W. *Comput. Phys. Commun.* **1991**, *63*, 691.
(66) Engel, V.; Schinke, R.; *J. Chem. Phys.* **1988**, *88*, 6831.